

1           **Suitability of static yield stress evolution to assess thixotropy of flowable**  
2   **cementitious materials**

3   Joseph J. Assaad

4    Dept. of Civil and Environmental Engineering, Notre Dame University, Zouk Mosbeh,

5    PO Box 72, Lebanon. E-mail: [jassaad@ndu.edu.lb](mailto:jassaad@ndu.edu.lb)

6   **ABSTRACT**

7    Behavior of self-consolidating concrete (SCC) after casting (such as stability, formwork  
8    pressure, and multi-layer interfaces) is directly affected by the flocculation aspect of  
9    thixotropy. The main objective of this paper is to evaluate the suitability of static yield  
10   stress ( $\tau_0$ ) evolution over time to assess the magnitude of thixotropy. Three series of  
11   highly flowable mortar mixtures were tested using the four-bladed vane method, and the  
12   results were compared with the cohesion ( $C$ ) values obtained by direct shear. Test results  
13   have shown that  $\tau_0$  and  $C$  responses determined at given resting time are quite close to  
14   each other, indicating an adequate correlation between thixotropy determined using vane  
15   and direct shear methods. This reflects the suitability of considering  $\tau_0$  evolution over  
16   time to quantify the flocculation aspect of thixotropy, as well as its robustness as it is not  
17   affected by the testing method.

18   **Keywords:** Fresh concrete, Thixotropy, Four-bladed vane, Direct shear test.

19   **1.INTRODUCTION**

20   The successful casting of highly flowable self-consolidating concrete (SCC) entails  
21   proper knowledge and monitoring of thixotropic properties. For instance, the  
22   cementitious matrix should be easily deflocculated during agitation with reduced  
23   apparent viscosity, thus facilitating placement by gravity with improved passing ability

24 [1,2]. As soon as SCC placement is completed, the reversible phenomenon associated  
25 with the build-up of cementitious structure takes place over time. In vertical elements, a  
26 fast recovery is required as this improves stability and resistance towards aggregate  
27 segregation. Earlier studies showed that lack of stability can lead to surface defects,  
28 including bleeding and settlement that can weaken the quality of interface between  
29 aggregate and cement paste with direct effects on permeability, bond to steel, and  
30 mechanical properties [3,4]. Also, fast restructuring could be beneficial to reduce the  
31 SCC lateral stresses developed in vertical formworks [5].

32 In contrast, excessively high thixotropic SCC may not be appropriate when casting is  
33 made using injection or pumping techniques; i.e., if the material builds up its internal  
34 structure too fast and apparent yield stress exceeds a critical value, any stoppage (such as  
35 due to replenishment of buckets) may cause blockage of pipes and eventually abuse the  
36 equipment ultimate pressure in order to resume placement [1,2]. Also, high thixotropic  
37 SCC exhibiting fast structural recovery could not be appropriate during multi-layer  
38 casting in horizontal elements, as this creates cold joints and weak interfaces in the final  
39 structure. Some researchers reported mechanical and bond losses reaching 60% due to  
40 weak SCC interfaces [6,7].

41 Thixotropy of cementitious materials is often quantified by measuring the surface area  
42 during successive shear rate vs. stress measurements (Fig. 1). For example, because of the  
43 thixotropy transient and time-dependent nature, hysteresis loops are created when the  
44 plastic material is subjected to successive increasing/decreasing shear rates [1,2,5].  
45 During the increasing ramp, de-flocculation occurs but not fast enough for a steady state  
46 stress to be reached. The measured stress is thus higher than what would be obtained if

47 steady state was reached. During the decreasing ramp, flocculation occurs but again not  
48 fast enough for steady state to be reached, which creates the so-called hysteresis loops.  
49 Alternately, thixotropy can be quantified using the structural breakdown curves  
50 determined by subjecting the fresh material to given shear rate and recording stress  
51 variations over time [5]. The curves are typically characterized by peak yield stress that  
52 corresponds to the initial structural condition, and stress decay towards an equilibrium  
53 value (Fig. 1). Nevertheless, it is important to note that surface areas determined under  
54 dynamic conditions (i.e., hysteresis and structural breakdown curves) are highly  
55 dependent on the type of rheometer, testing protocol, applied shear rate, and flow history  
56 [2]. This prevents inter-laboratory comparison of test results and makes it difficult to  
57 assess the concrete properties using standardized testing protocols.

58 Under the concrete static condition after placement is completed, several authors studied  
59 the evolution of static yield stress ( $\tau_0$ ) over time [8,9,10], which would reflect the  
60 flocculation aspect of thixotropy and could be more relevant when assessing SCC  
61 behavior after casting especially the stability, formwork pressure, and multi-layer  
62 interfaces. The  $\tau_0$  is defined as the minimum stress required to initiate flow [11]; it  
63 reflects the physical restructuring of inter-particles links following a rest period coupled  
64 with attractive forces due to chemical reactions and formation of hydration compounds.  
65 The vane method is commonly used for measuring  $\tau_0$ , because of its simplicity and the  
66 possibility of preventing slip during shearing [2,5,9]. Its principle consists of inserting a  
67 four-bladed vane of diameter (D) and height (H) in the plastic material and recording at  
68 sufficiently low shear rate the maximum torque ( $T_m$ ) required to initiate flow.  
69 Considering the top edges of blades vane aligned with upper material surface (i.e., to

70 eliminate over-head stress contribution on torque measurements) and yielding occurring  
71 at the cylindrical surface defined by the blade tips [11,12],  $T_m$  can be written as:

$$72 \quad T_m = \left(\frac{\pi D^3}{2}\right) \left(\frac{H}{D} + \frac{1}{6}\right) \tau_0 \quad \text{Eq. 1}$$

73 When measurements are made at successive elapsed resting times after initial concrete  
74 mixing,  $\tau_0$  was found to increase linearly over time, which could be associated with the  
75 structuration rate of the cementitious matrix, as shown in Eq. 2:

$$76 \quad \tau_0(t_{\text{rest}}) = \tau_0(t_0) + A_{\text{Thix}} t_{\text{rest}} \quad \text{Eq. 2}$$

77 where  $t_{\text{rest}}$  is the resting time and  $A_{\text{Thix}}$  structuration rate (i.e., reflecting the magnitude of  
78 thixotropy) in Pa/s determined as the slope of tendency curve plotted between  $\tau_0(t_{\text{rest}})$  and  
79  $t_{\text{rest}}$ .

## 80 **2.USE OF DIRECT SHEAR TO ASSESS THIXOTROPY**

81 The direct shear test is widely used in soil mechanics to determine shear strength  
82 properties and analyze failure mechanisms occurring along interfaces. Its principle is  
83 quite simple, and consists of shearing two portions of a specimen by the action of steadily  
84 increasing force while constant load is applied normal to the plane of relative movement.  
85 Shear strength including cohesion (C) and angle of internal friction ( $\phi$ ) follow the Mohr-  
86 Coulomb law, given as:

$$87 \quad \tau = C + \sigma' \tan \phi \quad \text{Eq. 3}$$

88 where  $\tau$  and  $\sigma'$  refer to shear resistance and normal effective stress resulting from the  
89 solid grains, respectively.

90 In literature, the direct shear has often been employed as a reference test to develop and  
91 validate constitutive models characterizing the yield behavior of plastic materials. In fact,  
92 this test is standardized under ASTM D3080 [13] and available in most research centers;

93 it is realized under quasi-static conditions whereby shearing takes place within the  
94 material along pre-defined interface represented by the horizontal surface area of shearing  
95 box. This physically overcomes the complications related to wall slip, secondary flow,  
96 and confinement conditions encountered in conventional rheometers [2,12,14]. Alfani  
97 and Guerrini [15] reported that direct shear is particularly suited for rheological  
98 characterization and interfacial flow behavior between extrudable cohesive pastes and  
99 equipment forming wall systems. Lu and Wang [16] considered the direct shear test to  
100 validate a constitutive model developed for predicting yield stress of cementitious  
101 materials. The  $C$  determined by direct shear was found to be closely related to the “true”  
102  $\tau_0$  determined at low rotational speed using the four-bladed vane [10]. Recently, Assaad  
103 et al. [12] used the direct shear test to validate the effect of vane positioning on  $\tau_0$   
104 responses of freshly mixed cement pastes and poly-vinyl acetate emulsions possessing  
105 different flowability levels. Over-estimation of  $\tau_0$  occurred when the vane was inserted  
106 inside the specimen, particularly for cohesive materials. Conversely, positioning the vane  
107 blades flush with the upper specimen surface eliminated the contribution of material self-  
108 weight on torque measurements and resulted in close  $C$  and  $\tau_0$  values [12].

109 This paper is part of a comprehensive research project undertaken to provide new insights  
110 on various approaches used to quantify thixotropy of cementitious materials. It does not  
111 aim at substituting the vane method by direct shear, especially knowing that the vane  
112 method is widely used, simple, and versatile. Rather, the main objective of this paper is to  
113 evaluate the suitability and robustness of considering the evolution of  $\tau_0$  over time  
114 determined by vane method in order to quantify the magnitude of thixotropy. Three series  
115 of highly flowable mortar mixtures were tested using the vane method, and results

116 compared to those obtained by direct shear. Data presented in this paper can be of interest  
117 to researchers in various industries to facilitate inter-laboratory comparison and unify  
118 quantification of the flocculation aspect of thixotropy using standardized testing  
119 protocols.

## 120 **3.EXPERIMENTAL PROGRAM**

### 121 **3.1-Materials**

122 Portland cement and silica fume conforming to ASTM C150 Type I and C1240,  
123 respectively, are used. The surface areas of cement (Blaine) and silica fume (B.E.T.) were  
124 340 and 20,120 m<sup>2</sup>/kg, respectively; their specific gravities were 3.14 and 2.22,  
125 respectively. Continuously graded siliceous sand complying with ASTM C33  
126 specification was employed; its nominal particle size, fineness modulus, and bulk specific  
127 gravity were 4.75 mm, 2.42, and 2.63, respectively.

128 A polycarboxylate-based high-range water reducer (HRWR) complying with ASTM  
129 C494 Type F was incorporated in all mixtures. It had a specific gravity, solid content,  
130 alkali content, and pH of 1.1, 42%, 0.34%, and 6.2, respectively.

131 Liquid viscosity-modifying admixture (VMA) and thixotropy-enhancing agent (TEA)  
132 were used. The VMA is based on hydroxyethyl cellulose (HEC) ether with a specific  
133 gravity and solid content of 1.04 and 18%, respectively. It is commonly used for SCC  
134 production, with recommended dosage rates varying from 0.15% to 1% of cement mass.  
135 This VMA is produced by substituting number of hydroxyl groups within the cellulose  
136 backbone by functional groups to improve water solubility through a decrease in the  
137 molecule crystallinity. Its average weight molecular mass and degree of substitution are  
138 equal to 310 kDa and 1.8, respectively.

139 The TEA is an organic cyclic propylene carbonate (PC) compound produced from  
140 propylene oxide and carbon dioxide with a zinc halide catalyst. Its specific gravity and  
141 pH are 1.03 and 6.5, respectively, and recommended dosage for cement-based materials  
142 varies from 0.2% to 1.2% of cement mass. As will be discussed later, the use of TEA was  
143 necessary to increase the magnitude of  $A_{\text{Thix}}$  beyond 1 Pa/s; in fact, increasing the HEC-  
144 based VMA concentration to achieve higher thixotropic level is accompanied with  
145 considerably increased HRWR molecules to maintain similar flowability, thus delaying  
146 cement hydration reactions and extending setting times beyond 24 hours [17,18].  
147 Conversely, the delay in setting time was limited when the PC-based TEA was used in  
148 conjunction with HRWR.

### 149 **3.2-Mixture proportioning**

150 Three mortar series proportioned with cement quantities of 375, 435, and 500 kg/m<sup>3</sup> and  
151 water-to-cement ratio (w/c) of 0.46, 0.41, and 0.34, respectively, were considered (Table  
152 1). The mixtures were proportioned using the concrete-equivalent-mortar (CEM)  
153 approach; i.e., the cement content and w/c remained similar to those of corresponding  
154 concrete, except that all coarse aggregates are replaced by an equivalent quantity of sand  
155 in terms of specific surface area [19,20]. Aggregate-free CEM mixtures could better  
156 reflect the flocculation aspect of thixotropy, given that aggregates mostly affect internal  
157 friction that overshadows the build-up phenomenon of cementitious matrix [5,20].

158 A total of 12 CEM mixtures were tested. The silica fume, VMA, and TEA were added at  
159 relatively low to high dosage rates to achieve different  $A_{\text{Thix}}$  levels; i.e. silica fume at 5%  
160 or 10%, VMA at 0.35% or 0.8%, and TEA at 0.3% or 0.75% of cement mass (Table 1).  
161 In all mortars, the HRWR was adjusted to secure a flow of  $220 \pm 10$  mm when determined

162 as per ASTM C1437 (this flow corresponds to concrete slump flow of  $650 \pm 20$  mm  
163 determined using ASTM C143 slump cone) [21].

### 164 **3.3-Mixing and stability testing**

165 The mortar mixing procedure consisted of homogenizing the sand with half of mixing  
166 water, then introducing the cementitious materials gradually over 30 seconds. The  
167 remaining part of water along with the VMA or TEA along with HRWR were then added  
168 and mixed for 1.5 minutes. After a rest period of 30 seconds, the mortar was remixed for  
169 1.5 additional minutes. Testing and sampling were made at room temperature of  $23 \pm 2$  °C  
170 and  $50\% \pm 5\%$  relative humidity.

171 Right after mixing, the flow was measured by determining the material's average  
172 diameter after spreading on horizontal surface using a mini-slump cone having top  
173 diameter, bottom diameter, and height equal to 70, 100, and 50 mm, respectively [14].

174 The passing ability was evaluated using the Marsh cone having 12.7-mm outlet diameter;  
175 a volume of 500-mL was filled in the cone and allowed to rest for 5 seconds prior to flow  
176 time measurement. The bleeding was determined as per ASTM C232, and consists of  
177 measuring the relative quantity of mixing water that has bled from the fresh material  
178 placed in 75-mm diameter and 150-mm height container. For measurements, the  
179 container was slightly tilted and free water collected using a pipet from the specimen  
180 surface. The percentage of bleed water was obtained by dividing the collected water by  
181 the total mixing water in specimen.

### 182 **3.4-Assessment of $\tau_0$ using the four-bladed vane**

183 Right after mixing, the mortars were placed in 5 separate cylindrical recipients having  
184 each 120-mm height and 100-mm diameter for  $\tau_0$  measurements at 5 different  $t_{rest}$



185 intervals (i.e., at 0, 20, 40, 60, and 80 min). Anton Paar rheometer connected to four-  
186 bladed vane having 24-mm height and 12-mm diameter was used. For each measurement  
187 realized at given  $t_{rest}$ , the vane was gently introduced in the mortar in a way to position  
188 the top vane edges aligned with the upper material's surface. This was found particularly  
189 important when testing was realized at longer  $t_{rest}$  intervals of relatively moderate to high  
190 thixotropic mortars, as this avoided the material disturbance during the vane insertion  
191 process. It is to be noted that, prior to vane insertion, care was taken to tilt the recipient  
192 gently in order to remove using a pipette the eventual bleed water that occurred during  
193 the rest period (all mortars filled in recipients were covered by wet burlap during the rest  
194 period). The testing protocol consisted on subjecting the mortar to very low rotational  
195 speed of 0.3 rpm and recording the changes in torque as a function of time (mortars tested  
196 at  $t_0$  were allowed to rest for 1 min prior to testing).

### 197 **3.5-Assessment of C by direct shear**

198 An ELE Direct Shear apparatus complying with ASTM D3080 [13] was used for  
199 measuring  $C$  values of tested CEM (Fig. 2). The metal shear box measuring 100 mm  
200 diameter and 58 mm height is divided into two halves horizontally; the lower section can  
201 move forward at different constant velocities varying from 0.001 to 9 mm/min, while the  
202 upper section remains stationary. In order to eliminate friction between the two sections  
203 during movement and allow  $C$  measurements in the order of few Pa, four perfectly  
204 aligned 10-mm long channels were laser-grooved in the bottom part of the shear box [12].  
205 A steel ball having 2.5-mm diameter was then placed in each channel, thus allowing the  
206 lower plate of the shear box to behave like a roller with respect to the upper plate. The  
207 gap between both plates was  $10 \pm 1 \mu\text{m}$ , and filled with grease to avoid material's leakage.

208 The shear stresses were calculated by dividing the horizontal load by the specimen's  
209 cross-sectional area, i.e.  $7850 \text{ mm}^2$ . The complete description of direct shear test used can  
210 be seen in [12].

211 After mixing, the mortar was filled in the shear box and allowed to rest for the specified  
212 time interval (a new mortar was batched for each test). To alleviate the experimental  
213 program, 3 tests at different  $t_{\text{rest}}$  were realized for each mortar, except the 0.46-5%SF and  
214 0.41-5%SF mortars where 4 tests are conducted. The displacement rates were fixed at 0.5  
215 mm/min, a value found experimentally enough to overcome the restoring forces due to  
216 reorientation of particles and structural development due to cement hydration [12,22]. It  
217 is to be noted that the  $\phi$  parameter was not determined in this study, given that testing was  
218 realized without normal load applied on top of specimen during the shearing process.

## 219 **4.TEST RESULTS AND DISCUSSION**

### 220 **4.1-HRWR demand, setting times, and stability testing**

221 Table 2 summarizes the HRWR dosage needed to achieve flow of  $220 \pm 10$  mm along  
222 with the resulting unit weight, setting time, and stability indexes used to characterize  
223 CEM behavior. Briefly, the HRWR demand increased when mortars contained higher  
224 silica fume or VMA concentration. The increase in HRWR/VMA lengthened the setting  
225 time due to higher molecules adsorption onto cement particles that partly blocks the  
226 hydration reactions [17]. For example, the setting was delayed from 9:30 to 10:15 and  
227 14:15 hr:min for 0.46-5%SF, 0.46-10%SF, and 0.46-0.8%VMA, respectively. Mixtures  
228 containing TEA exhibited remarkably reduced setting times, as compared to equivalent  
229 mortars made with VMA.

230 As summarized in Table 2, the unit weights varied from  $1920 \pm 15$  to  $2050 \pm 30$  and  $2140$

231  $\pm 20 \text{ kg/m}^3$  for mixtures made with 0.46, 0.41, and 0.34 w/c, respectively. Generally  
232 speaking, the flow time increased with the reduction of w/c, particularly with the addition  
233 of silica fume or VMA, given the increased inter-particle friction and cohesiveness [2,3];  
234 values varied from 38 to 90 sec. Mortars incorporating TEA exhibited relatively moderate  
235 flow times of 73 sec, given that the mixture was not allowed to rest and build its structure  
236 prior to testing [17,18].

237 Typical variations in cumulative bleeding over time for selected mortars are given in Fig.  
238 3. Depending on CEM composition, the bleed water increased at different rates during the  
239 initial 20-min after placement, and tended to stabilize thereafter. For example, the  
240 bleeding rate decreased from 0.353 to 0.125 and 0.065 %/min for the 0.46-5%SF, 0.41-  
241 10%SF, and 0.34-0.35%VMA, respectively; the corresponding maximum bleed water  
242 determined after stabilization was 10.3%, 3.3%, and 1.5%, respectively. The 0.34-  
243 0.75%TEA mortar exhibited the lowest bleed rate and stabilized value, given its fast  
244 restructuring. Table 2 summarizes the bleeding rates determined over the initial 20-min  
245 and maximum bleed values obtained after stabilization.

#### 246 **4.2-The $\tau_0$ and C responses – Repeatability of testing**

247 Typical shear stress vs. horizontal displacement curves obtained by direct shear for  
248 selected mortars at different  $t_{\text{rest}}$  intervals are given in Fig. 4. As can be seen, the shear  
249 stress profiles showed linear elastic region until reaching the maximum peak value (taken  
250 as C). The presence of maximum value is an index of flocculation aspect of thixotropy  
251 that can be explained by the concept of structural build-up of bonds in the flocculated  
252 system [9,11,12]. Further horizontal displacement causes the stresses to decrease towards  
253 a steady state region. At maximum shear value, the horizontal displacement of bottom

254 shear box varied from 1 to 3 mm, depending mostly on  $t_{rest}$  interval. It is to be noted that  
255 the direct shear profiles are very similar to those typically obtained using the four-bladed  
256 vane [11,12,16], which reflects the similarity of both testing methods. The  $\tau_0$  and C  
257 values determined at various resting intervals are summarized in Table 3.

258 In order to evaluate repeatability of testing, three selected mortars possessing low to high  
259 thixotropic levels were tested 3 times using the vane and direct shear methods (a new  
260 batch was considered for each test). The coefficients of variation (COV) calculated as the  
261 ratio between standard deviation of responses and their mean values, multiplied by 100,  
262 are shown in Fig. 5. Generally speaking, the moderately thixotropic mixtures (i.e., 0.41-  
263 0.8%VMA) exhibited adequate repeatability, regardless of  $t_{rest}$  interval. Hence, the COV  
264 of various responses determined by the vane varied from 5% to 7.5% and from 4.6% to  
265 8.4% when using direct shear. The COV that resulted from direct shear increased up to  
266 11.7% and 15.4% at  $t_0$  for low and high thixotropic mixtures (i.e., 0.46-10%SF and 0.34-  
267 0.75%TEA, respectively). For the former category of mixtures, the increased COV can be  
268 related to reduced stability including bleeding and sedimentation, which affect variability  
269 of C responses. In contrast, the increased COV resulting from high thixotropic mixtures  
270 can be attributed to faster flocculation rates that make measurements quite sensitive to  
271 accuracy of testing procedures.

### 272 **4.3-Effect of mortar composition on $\tau_0$ and C**

273 The  $\tau_0$  measurements determined after mixing and 20 min later for tested mortars are  
274 plotted in Fig. 6. As expected, mortars prepared with combinations of increased cement  
275 content and reduced w/c led to higher  $\tau_0$  values, given the increased inter-particle links  
276 and reduced free mixing water. For example, such increase at  $t_0$  was from 39.4 to 53.2

277 and 63.3 Pa for the 0.46-5%SF, 0.41%-5%SF, and 0.34-5%SF, respectively. Also, for  
278 given w/c,  $\tau_0$  increased with the addition of silica fume (due to increased packing density  
279 of matrix) or VMA (due to polymer entanglement and hydrogen bonds) [2,3,7]. At longer  
280 elapsed resting times (i.e., at  $t_{20}$ ), all mortars exhibited increased  $\tau_0$  responses, depending  
281 on the flocculation rate associated with cement hydration reactions that occurred during  
282 the rest period.

283 It is interesting to note that relatively low  $\tau_0$  values were determined right after mixing  
284 (i.e., at  $t_0$ ) for mortars containing TEA, but then significantly increased over time. For  
285 example,  $\tau_0$  of 0.34-0.75%TEA was 50.3 Pa at  $t_0$ , but reached the highest value of 1106  
286 Pa at  $t_{20}$ . This clearly reflects the thixotropic mode of action of this agent through which  
287 the physico-chemical interactions of propylene carbonate with cement particles lead to  
288 significant structural build-up at rest with increased  $\tau_0$  responses [17,18].

289 ***Comparison with C values*** – With the exception of 3 mortars made with 0.46-w/c  
290 possessing unstable nature (i.e., 0.46-5%SF, 0.46-10%SF, and 0.46-0.35%VMA), the  
291 order of C magnitude determined by direct shear at given  $t_{rest}$  was pretty close to that of  
292 corresponding  $\tau_0$  (Table 3); the measurements remained within the repeatability of  
293 testing. In the case of unstable mortars, the C values determined after certain  $t_{rest}$  were  
294 higher by around 1.5 to 2.5 times than corresponding  $\tau_0$ . For instance, the C of 0.46-  
295 5%SF mortar registered after 20, 40, and 60 min rest was 146, 363.5, and 612.7 Pa,  
296 respectively; while corresponding  $\tau_0$  was 85.7, 146.2, and 271 Pa, respectively. This  
297 could be related to reduced stability, including bleeding and sedimentation that increase  
298 concentration of solid particles towards the lower half of the shearing box where  
299 interfacial failure plane is expected to occur, thus leading to increased shear stresses. The

300 difference in material concentration was felt when trying to move a spatula manually  
301 from the top surface to interfacial region in the shearing box [12].

302 The relationships between  $\tau_0$  and C responses for all tested mortars measured at various  
303  $t_{rest}$  along with their correlation coefficients ( $R^2$ ) are given below (the relationships were  
304 forced to intercept the origin of axis, thus having the form  $y = A x$ ).

305 At  $t_0$ :  $C = 1.104 \tau_0$   $R^2 = 0.82$  Eq. 4

306 At  $t_{20}$ :  $C = 0.964 \tau_0$   $R^2 = 0.92$  Eq. 5

307 At  $t_{40}$ :  $C = 0.905 \tau_0$   $R^2 = 0.97$  Eq. 6

#### 308 **4.4-The $A_{Thix}$ values determined by different methods**

309 Typical example showing the determination of  $A_{Thix}$  by considering the slope of tendency  
310 curves of  $\tau_0$  or (C value) determined at various  $t_{rest}$  using the vane or direct shear methods  
311 is given in Fig. 7; the results obtained are summarized in Table 3. Clearly, the  $\tau_0$  and C  
312 values followed increasing trends with resting time, depending on mortar constituents and  
313 ability to restructure skeleton at rest. The  $R^2$  of all tendency curves were higher than 0.95,  
314 reflecting that both methods can appropriately be used to assess  $A_{Thix}$  of cementitious  
315 materials.

316 The effect of CEM composition on  $A_{Thix}(\tau_0)$  magnitudes is shown in Fig. 8. Following the  
317 same phenomena described earlier,  $A_{Thix}(\tau_0)$  increased for mortars made with  
318 combinations of increased cement content and reduced w/c. For example, such increase  
319 was from 0.0682 to 0.143 and 0.575 Pa/s for the 0.46-5%SF, 0.41%-5%SF, and 0.34-  
320 5%SF, respectively. Also, for given w/c,  $A_{Thix}(\tau_0)$  increased with the addition of silica  
321 fume or VMA; at 0.41 w/c, this reached 0.178 and 0.892 Pa/s for 0.41-10%SF and 0.41-  
322 0.8%VMA, respectively. The highest  $A_{Thix}(\tau_0)$  of 1.172 and 1.484 Pa/s corresponded to

323 0.34-w/c mortars made with 0.3% or 0.75% TEA, respectively, mostly related to the  
324 thixotropic nature of this agent.

325 **Comparison with  $A_{Thix}(C)$  values** – As can be seen in Fig. 9, the ratio of  
326  $A_{Thix}(C)/A_{Thix}(\tau_0)$  varied from 1.5 to 2.5 for the unstable 0.46-5%SF, 0.46-10%SF, and  
327 0.46-0.35%VMA mortars. As previously explained, this can be related to reduced  
328 stability that over-estimated the shear stresses and resulted in higher  $A_{Thix}(C)$ .  
329 Subsequently, the  $A_{Thix}(C)/A_{Thix}(\tau_0)$  ratio hovered around 1.0 for all other CEM, implying  
330 that the magnitude of  $A_{Thix}$  becomes almost similar for relatively stable mixtures,  
331 regardless of testing method. This reflects the accuracy of considering the slope of  $\tau_0$   
332 determined at various  $t_{rest}$  to quantify the flocculation aspect of thixotropy, as well as its  
333 robustness as it is not affected by the testing method. The relationship between both  
334 indices for all tested mortars is given as:

$$335 \quad A_{Thix}(C) = 0.884 A_{Thix}(\tau_0) \quad R^2 = 0.97 \quad \text{Eq. 7}$$

336 The relationships between  $\tau_0$  or C responses determined after mixing (i.e., at  $t_0$ ) and  
337 corresponding magnitude of  $A_{Thix}$  are plotted in Fig. 10. If excluding mortars prepared  
338 with TEA, it is interesting to note that  $\tau_0$  determined by the vane method can well be used  
339 to predict  $A_{Thix}(\tau_0)$  with acceptable  $R^2$  of 0.82. Mixtures containing TEA exhibited  
340 moderate  $\tau_0$  values at  $t_0$ , albeit their rates of increase were significantly accentuated. A  
341 relatively moderate  $R^2$  of 0.54 resulted from C determined by direct shear right after  
342 mixing and corresponding  $A_{Thix}(C)$  data.

## 343 **5.CONCLUSIONS**

344 Monitoring the flocculation aspect of thixotropy is essential to predict SCC properties  
345 after casting such as stability, formwork pressure, and multi-layer interfaces. The main

346 objective of this paper is to evaluate the suitability of  $\tau_0$  evolution over time determined  
347 by vane method in order to assess the magnitude of thixotropy. Three series of highly  
348 flowable mortars were tested using a four-bladed vane, and results compared to C values  
349 obtained by direct shear. Standardized under ASTM D3080 and available in most  
350 research centers, the direct shear can be considered as a reference test to unify  
351 quantification and validate constitutive models intended for yield behavior of  
352 cementitious materials.

353 Based on the foregoing, test results from this study showed that  $\tau_0$  and C values increased  
354 when mixtures are prepared with reduced w/c and/or addition of silica fume or VMA.  
355 The TEA led to remarkably high  $\tau_0$  and C values, given the fast build-up of cementitious  
356 matrix. The  $A_{\text{Thix}}(C)/A_{\text{Thix}}(\tau_0)$  ratio varied from 1.5 to 2.5 for low thixotropic and  
357 unstable mortars, which was attributed to bleeding and sedimentation that alter  
358 concentration of solid particles where interfacial failure is expected to occur. In contrast,  
359  $A_{\text{Thix}}(C)/A_{\text{Thix}}(\tau_0)$  ratio hovered around 1.0 for stable mixtures, reflecting similar  
360 magnitudes of thixotropy. Adequate correlation exists between thixotropy determined by  
361 four-bladed vane and direct shear methods. This reflects the suitability of considering the  
362 slope of  $\tau_0$  determined at various rest intervals to quantify thixotropy, as well as its  
363 robustness as it is not affected by the testing method.

#### 364 **CONFLICT OF INTEREST**

365 The author declares that there is no conflict of interest regarding the publication of this  
366 paper.

#### 367 **REFERENCES**

368 [1] Wallevik JE. Rheological properties of cement paste: Thixotropic behavior and



369 structural breakdown. *Cement and Concrete Research*. 2009; 39:14-29.

370 [2] RILEM Technical Committee, Final report of RILEM TC 188-CSC. Casting of self-  
371 compacting concrete. *Materials and Structures*. 2006; 39:937-954.

372 [3] Assaad JJ, Khayat KH, Daczko J. Evaluation of static stability of self-consolidating  
373 concrete. *ACI Materials Journal*. 2004; 101(3):168-176.

374 [4] Zhu W, Gibbs JC, Bartos PJM. Uniformity of in-situ-properties of self-compacting  
375 concrete in full-scale structural elements. *Cement and Concrete Composites*. 2001;  
376 23(1):57-64.

377 [5] Assaad JJ, Khayat KH. Effect of coarse aggregate characteristics on lateral pressure  
378 exerted by self-consolidating concrete. *ACI Materials Journal*. 2005; 102(3):145-153.

379 [6] Roussel N, Cussigh F. Distinct-layer casting of SCC: The mechanical consequences  
380 of thixotropy. *Cement and Concrete Research*. 2008; 38:624-632.

381 [7] Assaad JJ, Issa C. Preliminary study on interfacial bond strength due to successive  
382 casting lifts of self-consolidating concrete – Effect of thixotropy. *Construction and*  
383 *Building Materials*. 2016; 126:351-360.

384 [8] Billberg P. Form pressure generated by self-compacting concrete – Influence of  
385 thixotropy and structural behaviour at rest. Ph.D. thesis, Dep. of Structural Engineering,  
386 The Royal Institute of Technology, Stockholm, 2006.

387 [9] Roussel N. Rheology of fresh concrete: from measurements to predictions of casting  
388 processes. *Materials and Structures*. 2007; 40:1001-1012.

389 [10] Assaad JJ. Correlating thixotropy of self-consolidating concrete to stability,  
390 formwork pressure, and multi-layers casting. *Journal of Materials in Civil Engineering*.  
391 2016; 28(10) DOI: 10.1061/(ASCE)MT.1943-5533.

392 [11] Nguyen QD, Boger DV. Direct yield stress measurement with the vane method.  
393 Journal of Rheology. 1985; 29:335-347.

394 [12] Assaad JJ, Harb J, Maalouf Y. Measurement of yield stress of cement pastes using  
395 the direct shear test. Journal of Non-Newtonian Fluid Mechanics. 2014; 214:18-27.

396 [13] ASTM D3080/D3080M-11. Standard Test Method for Direct Shear Test of Soils  
397 Under Consolidated Drained Conditions. ASTM Internatinoal, West Conshohocken, PA,  
398 2011.

399 [14] Barnes HA. A review of the slip (wall depletion) of polymer solutions, emulsions  
400 and particle suspensions in viscometers; its cause, character, and cure. Journal of Non-  
401 Newtonian Fluid Mechanics. 1995; 56:221-251.

402 [15] Alfani R, Guerrini GL. Rheological test methods for the characterisation of  
403 extrudable cement-based materials – a review. Materials and Structures. 2005; 38:239-  
404 247.

405 [16] Lu G, Wang K. Theoretical and experimental study on shear behavior of fresh  
406 mortar. Cement and Concrete Composites. 2011; 33:319-327.

407 [17] Assaad JJ, Daou Y. Cementitious grouts with adapted rheological properties for  
408 injection by vacuum techniques. Cement and Concrete Research. 2014; 59:43-54.

409 [18] Khayat KH, Assaad JJ. Use of thixotropy-enhancing agent to reduce formwork  
410 pressure exerted by self-consolidating concrete. ACI Materials Journal. 2008; 105(1):88-  
411 96.

412 [19] Schwartzentruher A, Catherine C. Method of the concrete equivalent mortar  
413 (CEM)—A new tool to design concrete containing admixture. (in French), Materials and  
414 Structures. 2000; 33:475-482.

415 [20] Assaad JJ, Khayat KH. Assessment of thixotropy of self-consolidating concrete and  
416 concrete-equivalent-mortar – Effect of binder composition and content. *ACI Materials*  
417 *Journal*. 2004; 101(5):400-408.

418 [21] Assaad JJ, Harb J, Chakar E. Relationships between key ASTM test methods  
419 determined on concrete and concrete-equivalent-mortar mixtures. *ASTM International*  
420 *Journal*. 2009; 6(3):1-14.

421 [22] Assaad JJ, Harb J, Maalouf Y. Effect of Vane Configuration on Yield Stress  
422 Measurements of Cement Pastes. *Journal of Non-Newtonian Fluid Mechanics*. 2016;  
423 230:31-42.

424

425

426

427  
428

**Table 1: Typical SCC classes and corresponding CEM composition**

	Typical classes of SCC mixtures		
Cement, kg/m <sup>3</sup>	375	435	500
w/c	0.46	0.41	0.34
Sand (0-4.75 mm), kg/m <sup>3</sup>	970	935	920
Aggregates (1.18-9.5 mm), kg/m <sup>3</sup>	825	795	780
Targeted slump flow, mm	650 ±20	650 ±20	650 ±20
	Tested mortars using the CEM approach		
Cement, kg/m <sup>3</sup>	375	435	500
w/c	0.46	0.41	0.34
Sand (0-4.75 mm), kg/m <sup>3</sup>	1065	1045	1010
Cement paste / sand, by volume	0.718	0.795	0.853
Silica fume, % of cement mass	0%, 5% and 10%		
VMA, % of cement mass	0%, 0.35%, and 0.8%		
TEA, % of cement mass	0%, 0.3%, and 0.75%		
HRWR, % of cement mass	Varies depending on CEM composition to achieve similar initial flow of 220 ±10 mm		

429  
430  
431

**Table 2: Effect of mortar composition on HRWR demand and stability indices**

	HRWR, % of cement	Initial flow, mm	Final set time, hr:min	Unit weight, kg/m <sup>3</sup>	Flow time, sec	Bleeding	
						Bleed rate, %/min	Max. bleed, %
0.46-5%SF	0.62	225	9:30	1910	38.25	0.353	10.3
0.46-10%SF	0.65	220	10:15	1930	40.45	0.235	8.5
0.46-0.35%VMA	0.65	225	11:45	1915	48	0.267	8.3
0.46-0.8%VMA	0.77	225	14:15	1930	63.5	0.14	5
0.41-5%SF	0.8	220	11:45	2080	49	0.165	4.2
0.41-10%SF	0.86	225	13:00	2050	52.25	0.125	3.3
0.41-0.35%VMA	0.85	220	15:00	2040	59.5	0.13	3.1
0.41-0.8%VMA	0.95	230	16:45	2065	80.25	0.085	2.1
0.34-5%SF	1.12	225	14:45	2145	86.25	0.095	2.3
0.34-0.35%VMA	1.1	230	15:30	2160	90	0.065	1.5
0.34-0.3%TEA	1.05	225	12:15	2130	72.5	0.047	0.9
0.34-0.75%TEA	1.05	230	12:45	2135	74	0.03	0.5

432 Mixture codification refers to: w/c - Percent and type of additive used (i.e., silica fume,  
433 VMA, or TEA)  
434  
435

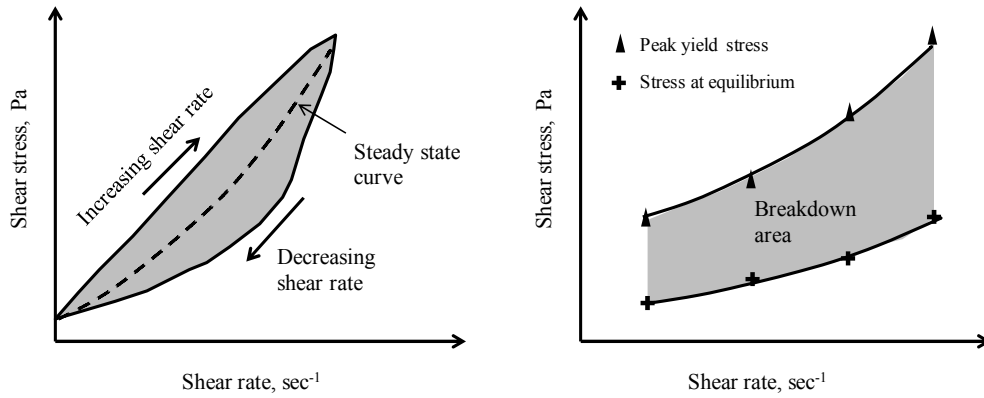
436  
437

**Table 3: Determination of  $A_{Thix}$  by four-bladed vane and direct shear**

	Four-bladed vane method		Direct shear method	
	$t_{rest}$ (min) and corresponding $\tau_0$ (Pa)	$A_{Thix}(\tau_0)$ , Pa/s	$t_{rest}$ (min) and corresponding C (Pa)	$A_{Thix}(C)$ , Pa/s
0.46-5%SF	$t_0 = 39.4$ ; $t_{20} = 85.7$ ; $t_{40} = 146.2$ ; $t_{60} = 271$ ; and $t_{80} = 355.8$	0.0682	$t_0 = 45.1$ ; $t_{20} = 146$ ; $t_{40} = 363.5$ ; and $t_{60} = 612.7$	0.16
0.46-10%SF	$t_0 = 42.6$ ; $t_{20} = 79$ ; $t_{40} = 200.8$ ; $t_{60} = 284$ ; and $t_{80} = 418$	0.0796	$t_0 = 41.8$ ; $t_{20} = 162$ ; and $t_{40} = 382$	0.142
0.46-0.35%VMA	$t_0 = 36.7$ ; $t_{20} = 101.4$ ; $t_{40} = 273$ ; and $t_{80} = 522.6$	0.105	$t_0 = 38$ ; $t_{20} = 186$ ; and $t_{30} = 360.4$	0.171
0.46-0.8%VMA	$t_0 = 45$ ; $t_{20} = 273$ ; $t_{60} = 881$ ; and $t_{80} = 1264$	0.254	$t_0 = 39.8$ ; $t_{10} = 171$ ; and $t_{30} = 559$	0.293
0.41-5%SF	$t_0 = 53.2$ ; $t_{20} = 183.5$ ; $t_{40} = 383$ ; and $t_{80} = 725.6$	0.143	$t_0 = 49$ ; $t_{20} = 174.5$ ; $t_{40} = 386$ ; and $t_{60} = 556$	0.144
0.41-10%SF	$t_0 = 48.3$ ; $t_{20} = 206$ ; $t_{40} = 415$ ; and $t_{60} = 691.2$	0.178	$t_0 = 55$ ; $t_{20} = 188.6$ ; and $t_{40} = 426$	0.154
0.41-0.35%VMA	$t_0 = 57.6$ ; $t_{20} = 422.1$ ; $t_{40} = 682$ ; and $t_{60} = 1274$	0.326	$t_0 = 57.1$ ; $t_{10} = 359$ ; and $t_{30} = 732$	0.366
0.41-0.8%VMA	$t_0 = 61$ ; $t_{20} = 428$ ; $t_{40} = 1806$ ; $t_{60} = 2844$ ; and $t_{80} = 4206$	0.892	$t_0 = 57.2$ ; $t_{10} = 429$ ; and $t_{30} = 1517$	0.825
0.34-5%SF	$t_0 = 63.3$ ; $t_{40} = 1308$ ; $t_{60} = 1802$ ; and $t_{80} = 2947$	0.575	$t_0 = 64.7$ ; $t_{40} = 1022$ ; and $t_{60} = 1905$	0.495
0.34-0.35%VMA	$t_0 = 67.3$ ; $t_{20} = 493$ ; $t_{40} = 1482$ ; $t_{60} = 2734$ ; and $t_{80} = 4033$	0.848	$t_0 = 70.4$ ; $t_{20} = 620$ ; and $t_{50} = 2408$	0.796
0.34-0.3%TEA	$t_0 = 51.2$ ; $t_{20} = 769$ ; $t_{40} = 2275$ ; and $t_{60} = 4238$	1.172	$t_0 = 58.3$ ; $t_{10} = 566$ ; and $t_{30} = 1894$	1.032
0.34-0.75%TEA	$t_0 = 50.3$ ; $t_{20} = 1106$ ; $t_{40} = 3275$ ; and $t_{60} = 5266$	1.484	$t_0 = 49.7$ ; $t_{20} = 985$ ; and $t_{40} = 2995$	1.227

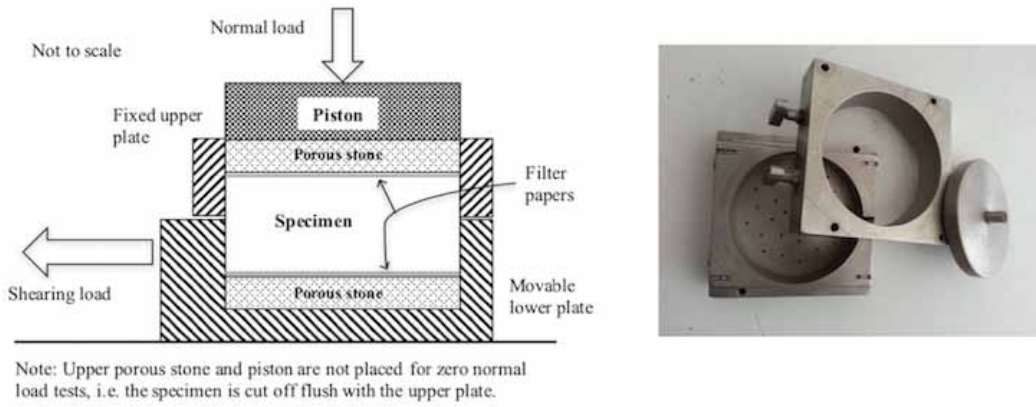
438  
439  
440  
441

442



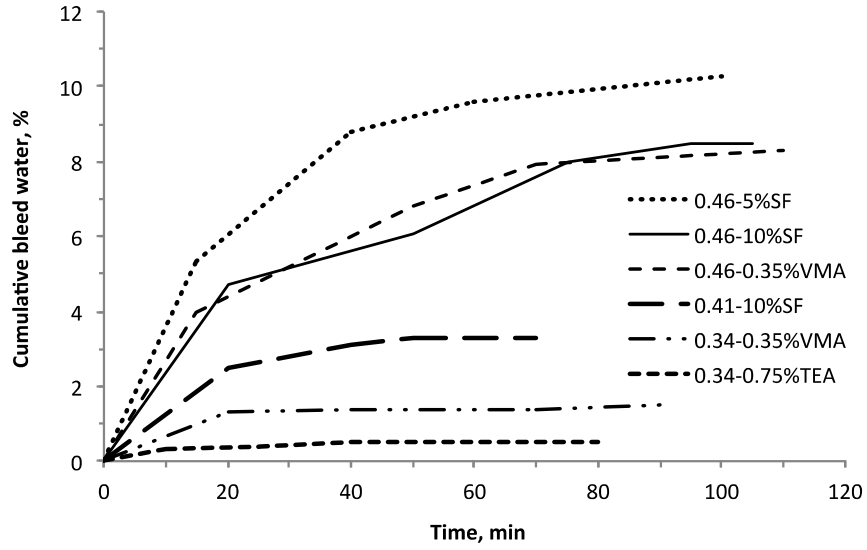
443  
444  
445  
446  
447  
448  
449  
450

**Fig. 1 Typical hysteresis loops and structural breakdown area for assessing the magnitude of thixotropy**



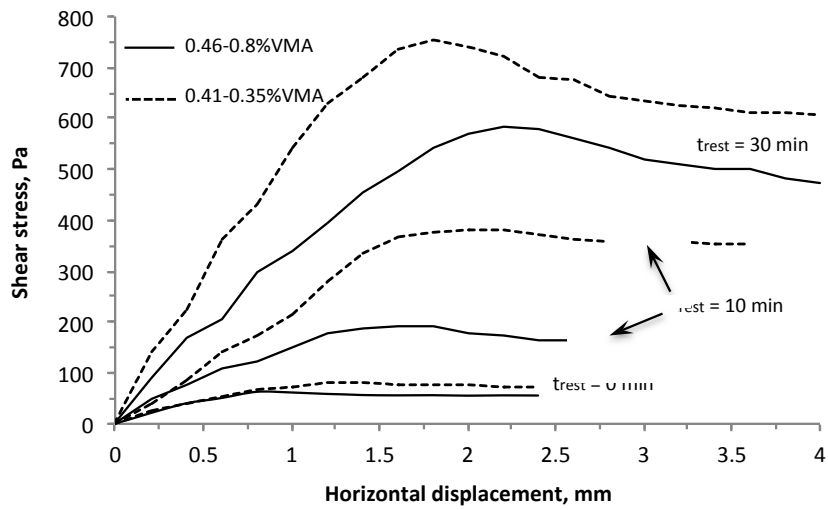
451  
452  
453  
454  
455

**Fig. 2 Photo for direct shear test**



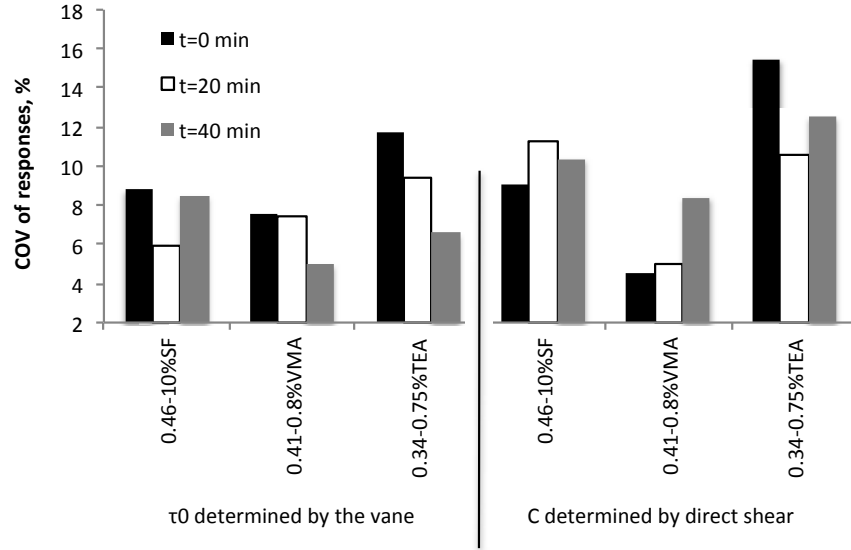
456  
457  
458  
459  
460  
461

**Fig. 3 Typical cumulative bleeding curves vs. time for selected mortars**



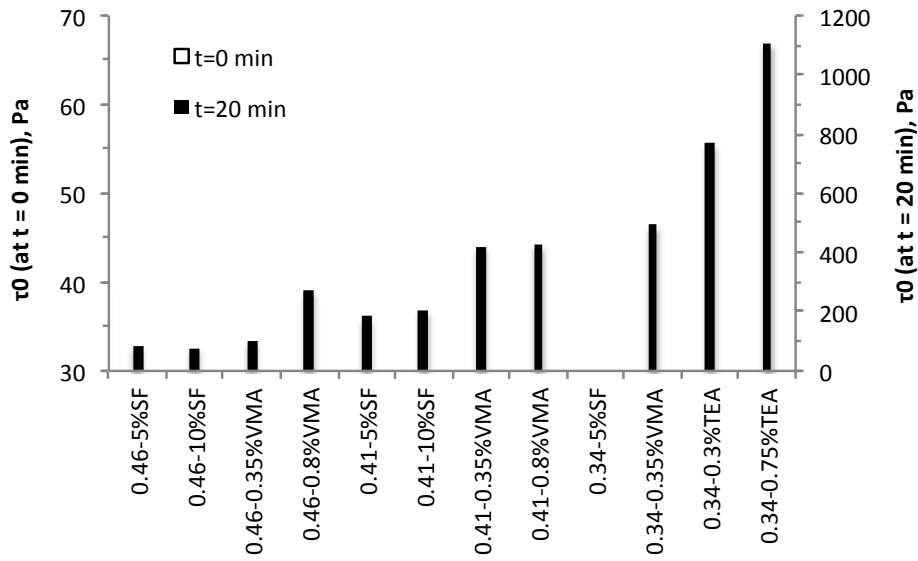
462  
463  
464  
465  
466  
467  
468

**Fig. 4 Typical shear stress vs. horizontal displacement plots determined at different  $t_{rest}$  by direct shear**



469  
470  
471  
472  
473  
474

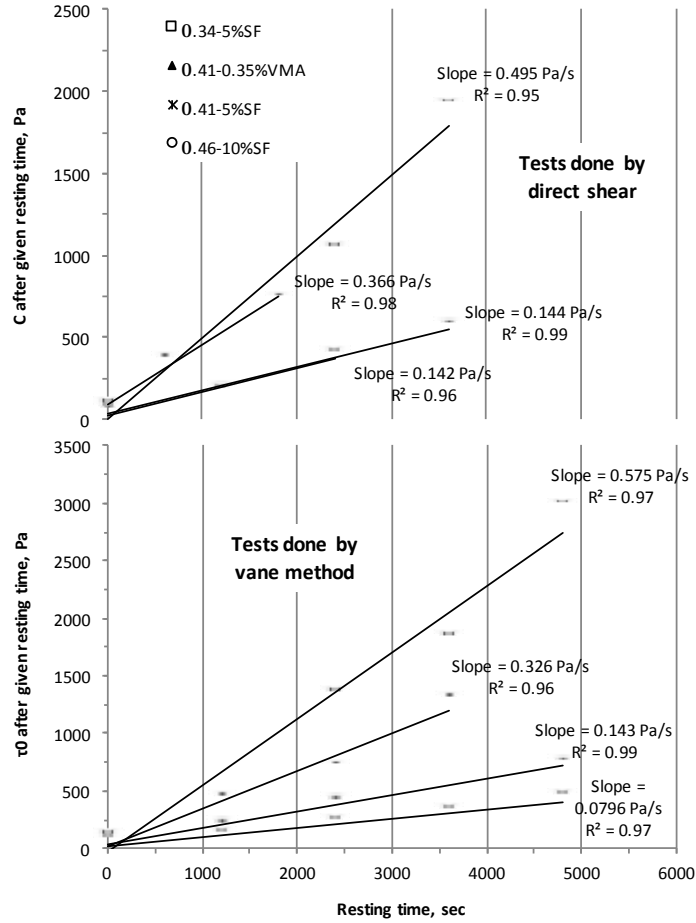
Fig. 5 COV of  $\tau_0$  and C responses determined at different  $t_{rest}$



475  
476  
477  
478  
479

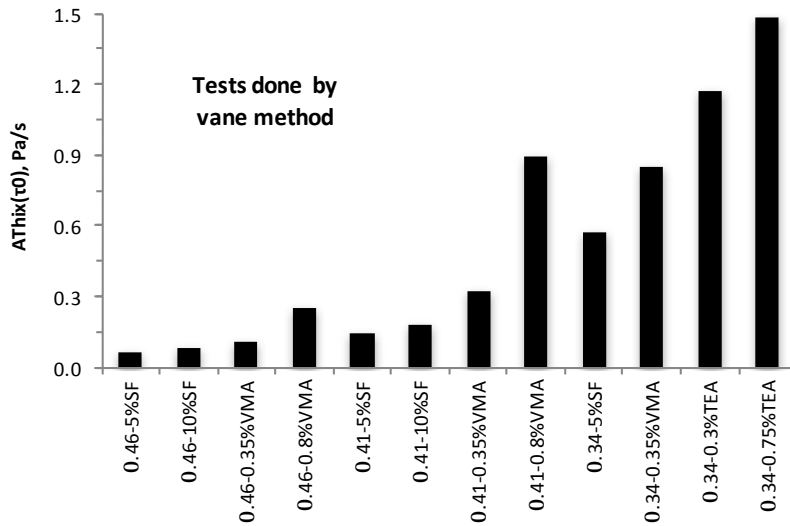
Fig. 6 Effect of mortar composition on  $\tau_0$  values determined at  $t_0$  and  $t_{20}$





480  
481  
482  
483  
484

**Fig. 7 Determination of  $A_{Thix}(\tau_0)$  and  $A_{Thix}(C)$  for selected mortars**



485  
486  
487  
488

**Fig. 8 Effect of mortar composition on  $A_{Thix}(\tau_0)$  measurements**

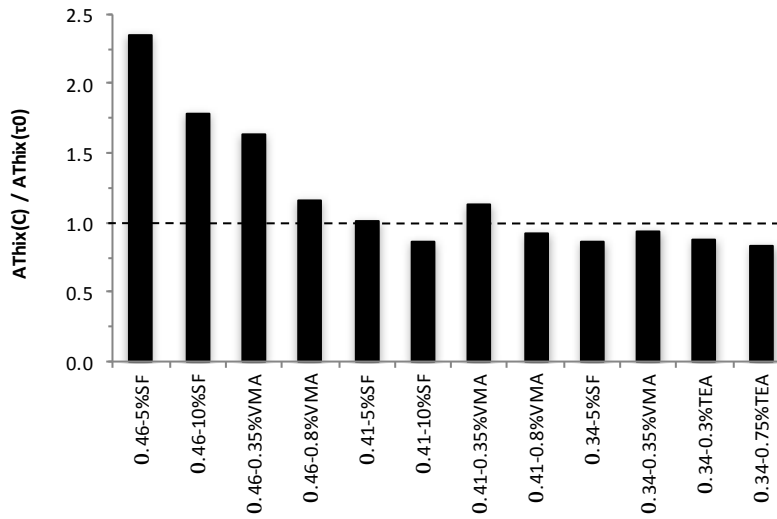


Fig. 9 Ratio between  $A_{Thix}(C)$  and  $A_{Thix}(\tau_0)$  measurements for tested mortars

490  
491  
492  
493  
494  
495

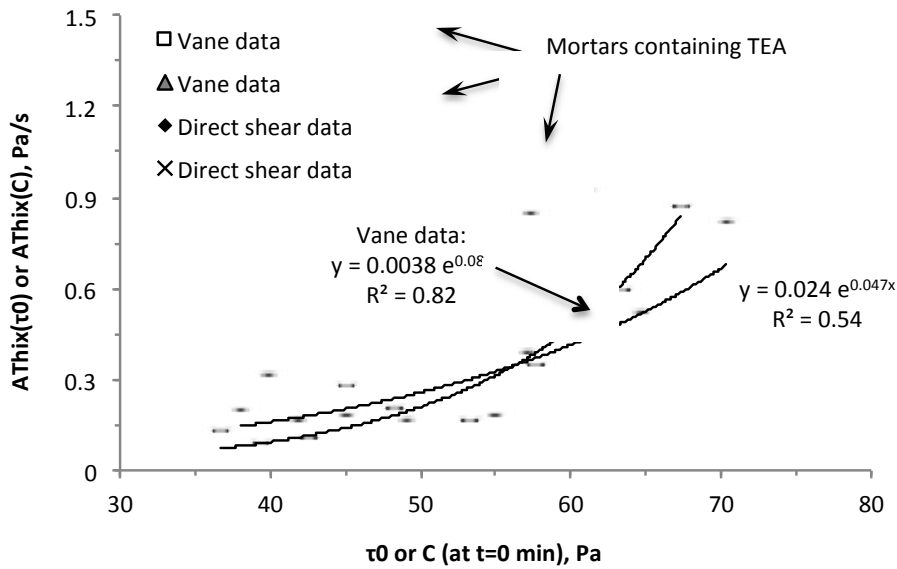


Fig. 10 Prediction of  $A_{Thix}(\tau_0)$  from  $\tau_0$  at  $t_0$  (and  $A_{Thix}(C)$  from  $C$  at  $t_0$ )

496  
497  
498  
499  
500  
501